red wild-type cells of one mating type by exposure to gamone of the other mating type in the presence of actinomycin $S_3$ (50 $\mu$g/ml) (Calbiochem), which does not inhibit the union of cells but prevents the separation of united cells. After 2 days, cells were fused in many pairs. When washed and cultured, some of them multiplied, keeping the fused condition. Three doublet clones of mating type 2 were thus obtained.

Homotypic unions of these doublets were induced in a mixture (98 : 1 : 1) of cell suspension, gamone 1 preparation (*11*), and 1 percent solution of bovine serum albumin (*12*). After 10 hours, when many homotypic complexes were formed, albinos of mating type 1 were added. Albinos started uniting to red complexes after 3 hours and remained united for about 2 days. Cells were fixed with Schaudinn's fluid 9, 14, 24, and 36 hours after the introduction of albinos, and were stained by the Feulgen reaction and light green.

Cells of *B. intermedium* have one long macronucleus and 10 to 30 micronuclei (about 1 $\mu$m in diameter) located near the macronucleus. In conjugation, micronuclei scatter in the cytoplasm, cells shrink, and nuclear cycles begin. The micronuclear cycles include three pregamic divisions: fertilization, repeated divisions of the fertilized nucleus, and differentiation of the division products to micronuclei and macronuclear anlagen. The macronuclear cycle includes the winding up, condensation, and degeneration of the old macronucleus and development of the new macronucleus from macronuclear anlagen (*13, 14*).

When a doublet unites with one or two albinos, all cells undergo macronuclear condensation and form macronuclear anlagen (Fig. 2A), indicating that nuclear cycles of conjugation regularly occur in doublet-albino mating.

In homotypic complexes to which no albinos unite, nuclei remain unchanged, except that micronuclei scatter in the cytoplasm and that the macronucleus winds up slightly in some cells (Fig. 1, C to E). However, if even a single albino cell unites to these homotypic complexes, most cells undergo macronuclear condensation and form macronuclear anlagen (Fig. 2B). When cells in a complex show different stages of the nuclear cycle, cells closer to the albino are in a more advanced stage (Fig. 2, C and F). It is therefore concluded that nuclear cycles begin in heterotypically united cells and propagate to other cells in the complex. This propagation is accompanied by a conspicuous shrinking of the cell (Fig. 2C), indicating that the cytoplasm is also undergoing a profound change.

The propagation of nuclear cycles is not mediated by the external medium, because the complexes without albinos never undergo nuclear cycles even if they are side by side with albino-united complexes for 36 hours. Thus an initiation factor of the nuclear cycle of conjugation which is produced by the heterotypically united cells and is transferred through cell unions may be postulated.

In some chain-type complexes in which an albino unites at one end, the macronuclear condensation is incomplete in cells at the other end, although new macronuclear anlagen are formed in the same cells (Fig. 2, D and E). This suggests that certain nuclear processes of conjugation might be controlled by different specific factors. In order to test this hypothesis, each factor should be isolated. A way to approach this problem would be to inject, by the microinjection method developed for *Paramecium aurelia* (*15*), fractionated samples from conjugating cells into a cell in the homotypic complex. The observed propagation of induced changes would be an assay of the activity of the factor. Such analysis would bring new insight into the regulation mechanism of the eukaryotic cell, especially the meiosis-initiating mechanism, because the first micronuclear cycle in ciliate conjugation is meiosis.

Doublets are known in other ciliates (*16*) including *P. aurelia* in which homotypic conjugation may occur (*2, 17*). However, in this species homotypically united cells also undergo all developmental changes of conjugation. The gamone-induced homotypic complex of *B. intermedium* is unique in that the process of conjugation stops at the stage of cell union, thus providing a test system for the isolation of factors that regulate meiosis and other nuclear and cytoplasmic events of conjugation and for analysis of their mode of transfer from cell to cell in multicellular complexes.

AKIO MIYAKE*
*Max-Planck-Institut für Molekulare Genetik, Berlin-Dahlem, Germany*

### References and Notes

1. T. M. Sonneborn, *Adv. Genet.* **1**, 263 (1947); K. G. Grell, *Protozoology* (Springer-Verlag, Berlin, 1973), pp. 199–225.
2. C. B. Metz, in *Sex in Microorganisms*, D. H. Wenrich, Ed. (AAAS, Washington, D.C., 1954), p. 284.
3. A. Miyake, *Curr. Top. Microbiol. Immunol.* **64**, 49 (1974).
4. ———, *Proc. Jpn. Acad.* **44**, 837 (1968).
5. ——— and J. Beyer, *Exp. Cell Res.* **76**, 15 (1973).
6. ———, *Science* **185**, 621 (1974).
7. Gamone 2, first named blepharismin (*8*), was renamed blepharismone (*3, 6*) to avoid terminological confusion [with the agreement of the authors of (*8*)].
8. T. Kubota, T. Tokoroyama, Y. Tsukuda, H. Koyama, A. Miyake, *Science* **179**, 400 (1973).
9. Supplied by Dr. F. Inaba, Nara University, Nara, Japan.
10. H. I. Hirshfield, I. R. Isquith, A. V. Bhandary, *J. Protozool.* **12**, 136 (1965); L. Chunosoff, I. R. Isquith, H. I. Hirshfield, *ibid.*, p. 459; *Blepharisma intermedium* was recently reclassified as *B. japonicum* v. *intermedium* [H. I. Hirshfield, I. R. Isquith, A. M. DiLorenzo, in (*14*), p. 304].
11. The gamone 1 preparation is a solution of partially purified blepharmone with the activity of $10^6$ unit/ml (*5*).
12. A protector of gamone 1 (*5, 6*).
13. S. Suzuki, *Bull. Yamagata Nat. Sci.* **4**, 43 (1957).
14. A. C. Giese, *Blepharisma* (Stanford Univ. Press, Stanford, Calif., 1973).
15. S. Koizumi, *Exp. Cell Res.* **88**, 74 (1974); J. K. C. Knowles, *ibid.*, p. 79.
16. T. M. Sonneborn, in *The Nature of Biological Diversity*, J. M. Allen, Ed. (McGraw-Hill, New York, 1963), p. 165.
17. K. Hiwatashi, in *Fertilization*, C. B. Metz and A. Monroy, Eds. (Academic Press, New York, 1969), vol. 2, p. 255.
18. Doublet culture often contains singlets which spontaneously arise from doublets.
19. I thank Drs. W. Messer and J. V. Bosch, Max-Planck-Institut für Molekulare Genetik, Berlin, for critically reading the manuscript, and A. M. Meyer, C. Hennig, and P. Hoppe for technical assistance.
* Present address: Istituto di Zoologia, Università di Pisa, Pisa, Italy.

17 October 1974

## Sleep Cycle Oscillation: Reciprocal Discharge by Two Brainstem Neuronal Groups

Abstract. *During the sleep cycle in cats, neurons localized to the posterolateral pole of the nucleus locus coeruleus and the nucleus subcoeruleus undergo discharge rate changes that are the opposite of those of the pontine reticular giant cells. The inverse rate ratios and activity curves of these two interconnected populations are compatible with reciprocal interaction as a physiological basis of sleep cycle oscillation.*

Neurons in the gigantocellular tegmental field (FTG) of the cat pontine brainstem show dramatic and state-specific discharge rate increases during desynchronized sleep (*1*). A tonic increase in discharge rate is detectable in the FTG population 5 minutes before the onset of desynchronized sleep (*2*), and phasic bursts of discharge by FTG neurons often lead the rapid eye movements of the fully developed desynchronized sleep episode by 250 msec (*3*). Neurons in most of the other tegmental nuclei share these properties of selectivity, tonic latency, and phasic latency with the FTG, although in diminishing degree as recording sites are distant from the FTG (*1–3*). These findings have led us to postulate that the FTG neurons may be a critical part of an executive system for desynchronized sleep and to consider pos-

sible cellular mechanisms underlying their periodic activation (*4*).

Progressive disinhibition of FTG units due to decreased activity of an inhibitory population is one possible mechanism, which might reveal itself in action potential data as decelerating activity curves at the onset of desynchronized sleep and by diminished discharge during desynchronized sleep. The recognition, localization, and characterization of pontine tegmental neurons with these two highly unusual discharge properties are the subjects of this report. The neurons showing discharge rate decreases in desynchronized sleep are found in the posteroventral pole of the nucleus locus coeruleus and in the nucleus subcoeruleus. Because some locus coeruleus (LC) neurons concentrate norepinephrine (*5*) and may use it as an inhibitory transmitter (*6*), we considered the possibility that LC cells might be functionally interacting with the giant cells during the sleep cycle and wished to test two predictions of that hypothesis—inverse discharge rate selectivity in desynchronized sleep and reciprocal time course of discharge rate change at the onset of each episode.

Table 1. Discharge rate data for tegmental nuclear neurons. Four cell groups are considered: LC, nucleus locus coeruleus and subcoeruleus; FTG, gigantocellular tegmental field; FTC, central, lateral, and paralemniscal tegmental fields; and TRC, tegmental reticular nucleus. For each group, arithmetic and geometric mean rates (in impulses per second) are presented for each of three behavioral states: W, waking; S, synchronized sleep; and D, desynchronized sleep. Selectivity ratios (D/W) are computed for each group using the geometric mean rates. Abbreviation: S.E.M., standard error of the mean.

| Computed value | W | S | D | D/W |
|---|---|---|---|---|
| | *LC cells* (N = *21*) | | | |
| Arithmetic mean rate ± S.E.M. | 7.25 ± 2.17 | 6.06 ± 1.71 | 6.27 ± 1.72 | |
| Cells decreasing rate (*N* = 13) | 8.75 ± 3.27 | 6.51 ± 2.53 | 2.81 ± 1.51 | |
| Cells increasing rate (*N* = 8) | 4.81 ± 2.20 | 5.33 ± 2.03 | 11.89 ± 2.92 | |
| Geometric mean rate | 3.08 | 2.79 | 0.969 | 0.314 |
| Cells decreasing rate (*N* = 13) | 4.06 | 2.56 | 0.256 | 0.0631 |
| Cells increasing rate (*N* = 8) | 1.97 | 3.19 | 8.42 | 4.27 |
| | *FTG cells* (N = *74*) | | | |
| Arithmetic mean rate ± S.E.M. | 5.95 ± 1.22 | 4.70 ± 0.915 | 17.8 ± 2.16 | |
| Geometric mean rate | 0.231 | 0.445 | 10.78 | 46.7 |
| | *FTC cells* (N = *32*) | | | |
| Arithmetic mean rate ± S.E.M. | 16.5 ± 4.59 | 15.0 ± 4.01 | 27.0 ± 5.42 | |
| Geometric mean rate | 1.21 | 1.66 | 10.9 | 9.02 |
| | *TRC cells* (N = *16*) | | | |
| Arithmetic mean rate ± S.E.M. | 13.4 ± 4.30 | 13.6 ± 3.47 | 29.1 ± 5.88 | |
| Geometric mean rate | 5.03 | 7.24 | 22.1 | 4.40 |

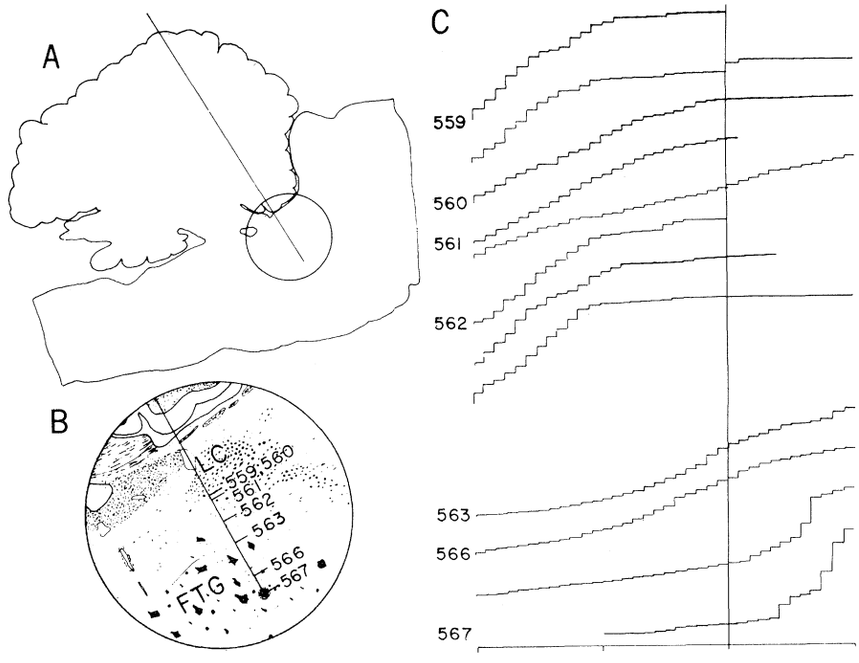


Fig. 1. Reciprocal discharge by cells in the nucleus locus coeruleus and gigantocellular fields of the anterior pontine tegmentum. (A) Outline tracing of a sagittal section of the cat pontine brain at 2.5 mm lateral to the midline, showing the path of an exploring microelectrode which passed through the anterior lobe of the cerebellum into the dorsal brainstem. (B) Detailed drawing of the histology in the zone circled in (A), showing the location of the seven successive recording sites in the penetration. The diameter of the circle is 5 mm. The cell fields of interest are labeled according to the terminology of Berman (*19*): LC, nucelus locus coeruleus; and FTG, gigantocellular tegmental field. (C) Cumulative rate histograms of the cells recorded at the seven sites shown in (B), during the transition period beginning 2 minutes before desynchronized sleep onset (vertical line) and ending 1 minute thereafter. Each activity curve shows the cumulative percentage of discharge for as much of the epoch as was free of arousal.

The data are extracellularly recorded action potentials from individual nerve cells of 25 male cats prepared for movable microelectrode explorations of the brainstem during natural sleep and waking. The methods of single cell recording, behavioral state identification, histological localization, and physiologic data analysis have been described in detail elsewhere (*1, 7*). In this report, we use selectivity ratios to quantify discharge density in desynchronized sleep with respect to waking and synchronized sleep; a selectivity ratio is determined by dividing the mean discharge rate in desynchronized sleep by that in either of the other two states (*8*). To quantify the time course of discharge rate change during transitions between sleep cycle states, we present cumulative histograms of individual and pooled cell discharge (*9*). Brief reports of these findings have been published elsewhere (*10*).

The microelectrode descent reconstructed in Fig. 1, A and B, is typical in that some of the cells with rate decreases in desynchronized sleep were clearly in the principal nucleus locus coeruleus, while others were in the more ventral nucleus subcoeruleus. For convenience we refer to all such neurons as LC cells. Spike height stability in multiple cycle recordings convinced us that these rate decreases (which sometimes ended in total arrest of discharge in desynchronized sleep) were real (Fig. 1C) and not the result of loss of spike discrimination.

The geometric mean discharge rate of 21 LC cells decreased moderately in transition from waking to synchronized sleep and fell more sharply still in desynchronized sleep (Fig. 2A). Comparable values for the FTG population showed opposite, nearly equal trends, the difference being a proportionately greater increase for the FTG population in desynchronized sleep. The inverse rate profiles gave rise to markedly different selectivity ratios (Fig. 2B). Discharge from FTG neurons is more

concentrated in desynchronized sleep than is discharge from LC neurons. As can be seen in Table 1, 13 of the 21 LC neurons had lowest discharge rates in desynchronized sleep, while none of the FTG cells did; in fact, only 4 of 128 cells localized to brainstem nuclei other than the locus coeruleus had lowest discharge rates in desynchronized sleep. The odds for chance occurrence of such disparate values are less than one in a billion (*11*).

Because of the possibility that the LC population contains two kinds of cell, one of which shares the properties of FTG cells while the other is distinctly different, we calculated and present in Table 1 the rate data for the LC subgroups as well as for the whole population. The threefold rate reduction over the cycle by the whole population of 21 LC cells was found to be five times again more marked in the subset of 13 neurons that decreased rate. By contrast, the selectivity ratios of cells which increased discharge rate were indistinguishable from those of cells in the tegmental reticular fields adjacent to the FTG. We thus believe that the LC population we have sampled contains two kinds of cell: one group, a minority, is like other pontine brainstem neurons in showing selectivity for desynchronized sleep, but this selectivity is relatively weak; the other group, a majority, is distinctly different, having a strong negative desynchronized sleep selectivity. In considering the time course of discharge activity of LC cells, we restrict our analysis to the latter group.

During the transition from the synchronized to the desynchronized phase of sleep, the trend of decelerating discharge rates of LC cells was opposite to the trend of accelerating rates of the FTG population: as LC neuronal discharge diminished, FTG neuronal discharge augmented. This is evident in Fig. 2C, where pooled transition data for LC neurons give a curve which approximates an inverse or mirror image of that determined by the data from FTG neurons.

We believe these findings to be of significance for theories of sleep cycle control since lesion, stimulation, and pharmacological experiments have implicated both the FTG and the LC zones as critical for the normal evolution of the sleep-waking cycle (*4*). More specifically, we see the results as relevant to the hypothesis that reciprocal interaction between functionally interconnected cell populations may determine the cyclical alternation of behavioral states. The FTG and LC cell groups are discretely localized, in direct spatial relation to one another, and possess reciprocal axodendritic contacts (*12*). These anatomical features, the reciprocal rate profiles,

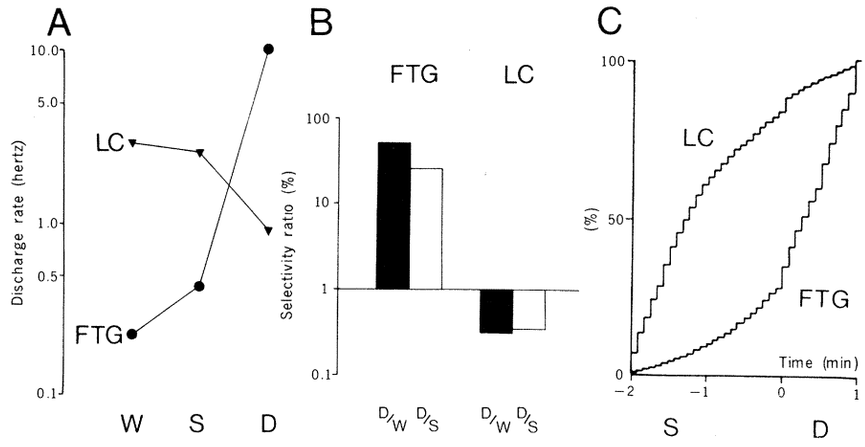


Fig. 2. Reciprocal rates, selectivity ratios, and sleep cycle activity curves for locus coeruleus (LC) and gigantocellular tegmental field (FTG) neurons. (A) Pooled geometric mean rates for population of 21 LC and 34 FTG neurons. Abscissas are three behavioral states: W, waking; S, synchronized sleep; and D, desynchronized sleep. (B) Selectivity ratios for the same pooled population data shown in (A). The ratios of geometric mean rate in D to that in W (solid bars) and in S (open bars) are plotted. (C) Pooled cumulative histograms of discharge rates in subsets of the two neuronal groups during the transition period from synchronized sleep to desynchronized sleep. Ordinates are percentages of discharges during the 3-minute time period (abscissas) beginning 2 minutes before and ending 1 minute after desynchronized sleep onset. The overall mirroring of the two curves suggests that the activity of the populations may be modulated by a shared, perhaps mutual process.

and the mirror image activity curves make functional interaction between the LC and FTG plausible.

We regard the possibility that the cells decreasing discharge rate in desynchronized sleep are norepinephrine-containing and inhibitory to the giant cells as a working hypothesis in view of the following observations. The mixed sleep cycle rate profiles in our LC data and Chu and Bloom's results (*13*) suggest that the LC may be functionally heterogeneous. However, Chu and Bloom found no cells with lowest discharge rates in desynchronized sleep among the 24 units recorded in fluorescent zones in the anterior and middle locus coeruleus. Thus, the identification of LC cells that decrease rate as norepinephrine-containing must be regarded as speculative*. Another possible source for giant cell inhibition is the dorsal raphe nucleus (DRN), where serotonin-containing neurons appear to be concentrated (*5*). A microwire recording study by McGinty and Harper (*14*) indicates that the DRN also contains many neurons which decrease discharge rate in desynchronized sleep. Anatomical evidence of fluorescence around giant cells is compatible with synaptic input from both serotonin- and norepinephrine-containing neurons (*15*), and thus either or both could mediate giant cell inhibition. We note the similarity of this aspect of our hypothesis to conclusions reached by others on the basis of pharmacological evidence (*16*).

Whatever the specific transmitters may be, reciprocal interaction between inhibitory and excitatory populations could account for the cellular data in the following way: during waking, FTG cells discharge rarely because they are tonically inhibited by the activity of cells of the LC type. At sleep onset, as LC activity and inhibition begin to wane, FTG neuronal discharge increases, at first minimally; with further disinhibition, FTG discharge progressively augments. At a critical point, perhaps associated with self-excitation in the FTG pool, the FTG neurons escape LC cell inhibition, and the subsequent exponential rise in FTG neuronal activity leads to desynchronized sleep onset (*2*). As FTG activity increases in the desynchronized phase peak, more and more activity is elicited in the LC population, whose inhibitory influence on FTG cells ends the desynchronized phase of sleep.

The reciprocal interaction theory is thus capable of ordering the cellular data to account for sleep cycle oscillation and, as shown by McCarley and Hobson (*17*), it does so in a manner amenable to detailed mathematical and physiological modeling. It also resolves much apparent contradiction in the lesion, stimulation, and pharmacological literature on sleep mechanisms, where each behavioral state tends to be viewed as a distinct entity controlled by its own center or its own chemical substance (*18*). More important still, the theory relates sleep control mechanisms to cellular electrophysiology and gives rise to specific and testable hypotheses of synaptic interconnections and the long-term modulation of their efficacy which may be a critical neural substrate of behavioral state control.

*Note added in proof: Since this report was accepted for publication, Chu and Bloom (*20*) have reported that 9 of 30 presumed norepinephrine-containing neurons in the LC region decreased rate in transition from the synchronized to the desynchronized phase of sleep.

J. ALLAN HOBSON
ROBERT W. MCCARLEY
PETER W. WYZINSKI
*Laboratory of Neurophysiology,*
*Department of Psychiatry,*
*Harvard Medical School,*
*Boston, Massachusetts 02115*

**References and Notes**

1. R. W. McCarley and J. A. Hobson, *Science* **174**, 1250 (1971); J. A. Hobson, R. W. McCarley, R. T. Pivik, R. Freedman, *J. Neurophysiol.* **37**, 497 (1974).
2. R. Freedman, J. A. Hobson, R. W. McCarley, R. T. Pivik, *Sleep Res.* **2**, 25 (1973); J. A. Hobson, R. W. McCarley, R. Freedman, R. T. Pivik, *J. Neurophysiol.* **37**, 1297 (1974).
3. J. A. Hobson, R. W. McCarley, R. T. Pivik, *Sleep Res.* **1**, 21 (1972); R. T. Pivik, J. A. Hobson, R. W. McCarley, *ibid.* **2**, 35 (1973); R. T. Pivik, R. W. McCarley, J. A. Hobson, in preparation.
4. J. A. Hobson, in *Advances in Sleep Research*, E. Weitzman, Ed. (Spectrum, New York, 1974), p. 217.
5. A. Dahlström and K. Fuxe, *Acta Physiol. Scand. Suppl.* **232**, 1 (1964).
6. M. Segal and F. E. Bloom, *Brain Res.* **72**, 79 (1974).
7. J. A. Hobson and R. W. McCarley, *Electroencephalogr. Clin. Neurophysiol.* **33**, 457 (19 → R. W. McCarley and J. A. Hobson, *ibid.* p. ← J. A. Hobson, *ibid.* **32**, 443 (1972).
8. In computing the geometric mean, neurons that did not discharge during the sample period were uniformly assigned a discharge rate of 0.0001 impulse per second.
9. Our cumulative histograms were constructed by summing the discharges occurring in successive 5-second epochs and expressing the values for each epoch as a percentage of the total number of counts in the 3-minute sample period.
10. J. A. Hobson, R. W. McCarley, P. W. Wyzinski, R. T. Pivik, *Sleep Res.* **2**, 29 (1973); *Program Abstr. Soc. Neurosci.* (1973), p. 373.
11. The probability was determined by the binomial test, conditioned on a true probability of twice the observed frequency of non-LC cells with lowest rates in desynchronized sleep.
12. M. E. Scheibel and A. B. Scheibel, in *Brain Information Service Conference Report No. 32* (Brain Information Service/Brain Research Institute, Los Angeles, 1973), p. 12.
13. N.-S. Chu and F. E. Bloom, *Science* **179**, 908 (1973).
14. D. J. McGinty and R. M. Harper, *Sleep Res.* **1**, 27 (1972).
15. F. E. Bloom, personal communication.
16. A. G. Karczmar, V. G. Longo, A. Scotti de Carolis, *Physiol. Behav.* **5**, 175 (1970); M. Jalfre, M. A. Ruch-Monachon, W. Haefely, in *Proceedings of the 1st Canadian International Symposium on Sleep*, Montreal, April 1972, pp. 155 → R. P. Simon, M. D. Gershon, D. C. Brooks, *Brain Res.* **58**, 313 (1973).
17. R. W. McCarley and J. A. Hobson, *Science* **189**, 58 (1975).
18. M. Jouvet, *Ergeb. Physiol. Biol. Chem. Exp. Pharmakol.* **64**, 166 (1972).
19. A. L. Berman, *The Brain Stem of the Cat* (Univ. of Wisconsin Press, Madison, 1968).
20. N.-S. Chu and F. E. Bloom, *J. Neurobiol.* **5**, 527 (1974).
21. We thank L. DiMatteo for histological assistance. Supported by NIMH grant MH 13,923.

12 November 1974; revised 25 February 1975

## Neuronal Excitability Modulation over the Sleep Cycle: A Structural and Mathematical Model

Abstract. *A model for control of the desynchronized phase of the sleep cycle postulates reciprocal interaction between cells in the pontine gigantocellular tegmental field (FTG cells) and cells in the nucleus locus coeruleus and nucleus subcoeruleus (LC cells). This physiological model leads to equations of the Lotka-Volterra type; the time course of activity predicted by the model is in good agreement with actual long-term recordings of FTG cells and single-cycle data for LC cells.*

The existence of a cell group in the region of the nucleus locus coeruleus (LC) of the cat with discharge activity curves opposite to those of cells in the gigantocellular tegmental field (FTG) has been documented by Hobson *et al.* (*1*). It was proposed that reciprocal interaction between excitatory and inhibitory neural populations may determine the alternation of sleep cycle states. We now present a simple structural and mathematical model for sleep cycle control based on the reciprocal interaction hypothesis and consider aspects of FTG and LC unit discharge activity curves in terms of the model (*2*).

The temporal organization of discharges in the FTG with respect to the sleep-waking cycle is illustrated in Fig. 1 for an FTG neuron recorded continuously for 10.5 hours. The most striking features of this discharge time course are the periodically occurring peaks of discharge activity, each of which corresponds to a desynchronized sleep episode. This regular, nonsinusoidal modulation of discharge activity was noticed in all of the six pontine reticular neurons recorded over 10 to 18 sleep-waking cycles (recording duration, 4.7 to 17.5 hours), although there was variability in the extent of modulation and cycle length. The presence of periodicity was confirmed by peaks in serial correlation coefficients and a dominant peak in the power spectral density (*3*).

For a detailed examination of the time course of discharge activity over the sleep-waking cycle, we normalized the duration of each cycle and averaged the activity over many cycles. Figure 2C presents the average activity curve for 12 cycles of FTG neuron 568, whose average cycle length was about 20 minutes. Note that the form of the activity curve is in general agreement with that in Fig. 1. What mechanism might be involved in generation of these nonsinusoidal, periodic neuronal activity curves? A detailed autocorrelation analysis of the discharge pattern of brainstem neurons gave no evidence for the regular, stereotyped discharge patterns generated by invertebrate pacemaker neurons involved in control of rhythmic activity (*4*). We were thus led to pursue the implications of the hypothesis that the time course of FTG unit activity is the result of reciprocal interaction with LC neurons.

Figure 2A shows the structural connections and the signs of influence that we have postulated. Golgi studies indicate the presence of FTG recurrent collaterals (*5*), and we have observed that the process of transition to high discharge levels in desynchronized sleep in FTG neurons is of exponential order, a finding compatible with self-excitation via such collaterals (*6*). Studies using Golgi (*7*) and Nauta (*8*) techniques have indicated the presence of a projection from FTG to LC cells which is postulated to utilize acetylcholine and to be excitatory. The available histochemical evidence points to the FTG cells as both using acetylcholine as a neurotransmitter and being influenced themselves by synaptically released acetylcholine (*9*). Connections from LC to FTG and from LC to LC cells are indicated by Golgi work (*7*) and by the presence of norepinephrine-containing varicosities in each area (*10*); these synapses are assumed to utilize norepinephrine as a neurotransmitter and to be inhibitory (*11*). Hobson *et al.* (*1*) discuss the problem of identification of the norepinephrine-containing cells with those recorded by us.

With this basic structural model, we proceeded to develop a parallel quantitative model of interaction. The mathematical form of terms describing the influence of each population on itself is suggested by evidence that the rate of change of activity levels in the FTG population is proportional to the current level of activity (*6*), and we propose that the same is true for the LC population, but with a negative sign because the recurrent feedback is inhibitory. The highly nonsinusoidal nature of FTG activity suggested that nonlinear FTG-LC interaction was to be expected. We model this effect by the simplest form of nonlinearity, the product of activities in the two populations; this is in accord with the reasonable physiological postulate that the effect of an excitatory or inhibitory input to the two populations will be proportional to the current level of discharge activity. Let $x(t)$ be the level of discharge activity in FTG cells; $y(t)$ the level of discharge activity in LC cells; and $a$, $b$, $c$, and $d$ positive constants identified with